

Hypoxia-Selective Targeting by the Bioreductive Prodrug AQ4N in Patients with Solid Tumors: Results of a Phase I Study

Mark R. Albertella,¹ Paul M. Loadman,⁴ Philip H. Jones,² Roger M. Phillips,⁴ Roy Rampling,⁵ Neil Burnet,³ Chris Alcock,⁶ Alan Anthoney,⁷ Egils Vjaters,⁸ Chris R. Dunk,¹ Peter A. Harris,¹ Alvin Wong,⁹ Alshad S. Lalani,⁹ and Chris J. Twelves⁷

Abstract Purpose: AQ4N is a novel bioreductive prodrug under clinical investigation. Preclinical evidence shows that AQ4N penetrates deeply within tumors and undergoes selective activation to form AQ4, a potent topoisomerase II inhibitor, in hypoxic regions of solid tumors. This proof-of-principle, phase I study evaluated the activation, hypoxic selectivity, and safety of AQ4N in patients with advanced solid tumors.

Experimental Design: Thirty-two patients with cancer (8 glioblastoma, 9 bladder, 8 head and neck, 6 breast, and 1 cervix) received a single 200 mg/m² dose of AQ4N before elective surgery. AQ4 and AQ4N levels in 95 tissues (tumor, healthy tissue) were assessed by liquid chromatography-tandem mass spectrometry. Tissue sections were also analyzed for AQ4 fluorescence using confocal microscopy, and for expression of the hypoxia-regulated glucose transporter, Glut-1.

Results: Activated AQ4 was detected in all tumor samples with highest levels present in glioblastoma (mean 1.2 µg/g) and head and neck (mean 0.65 µg/g) tumors; 22 of 32 patients had tumor AQ4 concentrations ≥0.2 µg/g, levels previously shown to be active in preclinical studies. In 24 of 30 tumor samples, AQ4 was detected at higher concentrations than in adjacent normal tissue (tumor to normal ratio range 1.1-63.6); distant skin samples contained very low concentrations of AQ4 (mean 0.037 µg/g). Microscopic evaluation of tumor sections revealed that AQ4 colocalized within regions of Glut-1 + hypoxic cells.

Conclusions: AQ4N was activated selectively in hypoxic regions in human solid tumors. Intratumoral concentrations of AQ4 exceeded those required for activity in animal models and support the evaluation of AQ4N as a novel tumor-targeting agent in future clinical studies.

It is well recognized that the abnormal vasculature of most solid tumors results in the poor delivery of oxygen and nutrients to localized regions within tumors (1–4). These regions of low oxygen concentration (hypoxia) are characteristic of many solid tumors, in contrast to healthy tissue, which is well vascularized. Hypoxia triggers changes in the transcrip-

tional regulation of a plethora of genes involved in cellular metabolism, angiogenesis, and metastasis, further propagating tumor growth and spread (1, 5–7).

Hypoxic tumor cells are resistant to radiotherapy as well as cytotoxic agents (4, 8–11). Several mechanisms contribute to this, including direct requirement of oxygen for ionizing radiation damage, reduced penetration and delivery of chemotherapeutic agents, and the protective effects of hypoxia-regulated genes. These factors, coupled with the increased genetic instability observed in hypoxic cells, facilitate the selection of resistant clones, tumor repopulation, and treatment failure (12–14). Indeed, the expression of hypoxia-regulated markers such as the glucose transporter-1 (Glut-1) has been associated with poor prognosis and/or treatment failure in a range of solid tumors (15–19). There is, therefore, a strong rationale for the development of novel agents that specifically target treatment-resistant and hypoxic regions of tumors with minimal toxicity to normal tissues.

One such agent under clinical investigation is AQ4N (banoxantrone; 1,4-bis {[2-(dimethylamino)ethyl]amino}-5,8-dihydroxyanthracene-9, 10-dione bis-*N*-oxide), a novel prodrug that was designed to be activated to a potent cytotoxin in hypoxic tumor regions (20–23). It is postulated that the combination of AQ4N with conventional therapeutic agents may facilitate the targeting of both normoxic and hypoxic

Authors' Affiliations: ¹KuDOS Pharmaceuticals, Ltd., ²Medical Research Council Cancer Cell Unit and Hutchison-Medical Research Council Research Centre, and ³University of Cambridge and Addenbrooke's Hospital, Cambridge, United Kingdom; ⁴Institute of Cancer Therapeutics, University of Bradford, West Yorkshire, United Kingdom; ⁵Beatson West of Scotland Cancer Centre, Glasgow, Scotland, United Kingdom; ⁶Oxford Radcliffe Hospitals, Oxford, United Kingdom; ⁷University of Leeds and Cancer Research UK Clinical Centre, St. James Hospital, Leeds, United Kingdom; ⁸Paul Stradiņš University Hospital, Riga, Latvia; and ⁹Novacea, Inc., South San Francisco, California

Received 8/25/07; revised 10/17/07; accepted 10/21/07.

Grant support: KuDOS Pharmaceuticals, Ltd., and Novacea, Inc.

The costs of publication of this article were defrayed in part by the payment of page charges. This article must therefore be hereby marked *advertisement* in accordance with 18 U.S.C. Section 1734 solely to indicate this fact.

Note: Supplementary data for this article are available at Clinical Cancer Research Online (<http://clincancerres.aacrjournals.org/>).

Requests for reprints: Alshad S. Lalani, Novacea, Inc., 400 Oyster Point Boulevard, Suite 200, South San Francisco, CA 94080. Phone: 650-228-1882; Fax: 650-228-1087; E-mail: lalani@novacea.com.

©2008 American Association for Cancer Research.
doi:10.1158/1078-0432.CCR-07-4020

regions of the tumor microenvironment. Indeed, AQ4N has been shown to enhance the therapeutic response to radiation (24, 25), cisplatin (25, 26), and other chemotherapies (25, 27, 28) in preclinical models.

AQ4N is relatively nontoxic until it is bio-reduced in hypoxic cells by a two-step enzymatic reduction to form AQ4M, a short-lived mono-*N*-oxide intermediate, and then to the ditertiary cationic amine, AQ4, which is a potent cytotoxin. AQ4, but not AQ4N, intercalates DNA with high affinity and functions as a potent inhibitor of topoisomerase II (29). Bio-reduction of AQ4N occurs strictly in the absence of oxygen and seems to be catalyzed by a number of cytochrome P450 (CYP) enzymes (30–32), which are commonly up-regulated in tumors (33–35). The high-affinity DNA binding limits diffusion of AQ4 outside of the tumor microenvironment, resulting in minimal systemic toxicity. Moreover, early clinical trials have shown that AQ4N is well-tolerated in patients without evidence of any major systemic toxicities at doses up to 447 mg/m² when given in combination with radiation (36) or 768 mg/m² given weekly as a single agent (37). In this study, patients received a single 200 mg/m² dose of AQ4N as this represented a margin of substantial safety before surgery.

This translational, proof-of-principle study was designed to establish whether AQ4N was preferentially activated in tumors rather than normal tissue, and whether the activated AQ4 metabolite selectively accumulated in hypoxic regions. A spectrum of solid tumor and normal tissues were biopsied following scheduled surgical resection and examined for levels of the AQ4N prodrug and its activated form, AQ4, using mass spectrometry. In addition, the tissue distribution of AQ4 in relation to tumor hypoxia was assessed using confocal microscopy and by immunohistochemical detection of the Glut-1 hypoxia marker.

Materials and Methods

Patient selection. Patients with histologic or cytologic confirmation of malignancy, who were candidates for elective surgery for tumor removal or reduction, were eligible; for glioblastoma multiforme (GBM) patients, a firm radiological diagnosis was accepted. Patients were required to be ≥18 years of age; with adequate bone marrow, liver, and kidney reserve; and to have provided written informed consent. Patients were ineligible if they had received radiotherapy (except limited field palliative treatment), endocrine therapy, immunotherapy, or chemotherapy treatment; or if they had received major thoracic/abdominal surgery within 4 weeks of study entry; patients were also required to have recovered from reversible toxicities of any prior therapy. Patients with evidence of peripheral or central cyanosis, any history of serious or uncontrolled ischemic heart disease, peripheral cerebrovascular disease, or nonspecific chest pain were all ineligible. Pregnant or lactating women were not eligible.

Study design, dosage, and drug administration. Patient history, physical examination, electrocardiogram, and routine clinical laboratory studies were conducted within 14 days of drug administration. Each patient received a single 200 mg/m² dose of AQ4N by i.v. infusion over ~30 min. No other cytotoxic medication was administered.

AQ4N was provided in vials containing 150 mg AQ4N as the free base. Each vial was reconstituted with sterile water to achieve a concentration of 25 mg/mL. The reconstituted solution was mixed aseptically with 250 mL 0.9% NaCl solution and infused through an inline filter.

Tumor biopsy sampling and procedure. Approximately 12 to 36 h following AQ4N administration, multiple samples of tumor and

normal tissue (if available) were surgically resected from each patient. Tissue specimens were washed thrice in ice-cold 0.9% NaCl solution, blotted, and frozen in liquid N₂ and stored at -80°C pending analysis. The mean time of delay from resection of tissues to freezing was ~2 min. Samples were divided and analyzed for drug levels by mass spectral analysis and for hypoxia using immunohistochemical staining as described below.

Pharmacokinetic sampling and assays. Blood samples were collected immediately before the end of AQ4N infusion and just before the surgical resection. AQ4N, AQ4M, and AQ4 were extracted from plasma using MCX solid phase extraction well plates (Waters Corporation) and separated by reverse-phase high-performance liquid chromatography using an Astec polymer C18 column as previously described (38, 39). Each compound was detected using a tandem quadrupole mass spectrometer. The linear range for the assay was 10 to 2,000 ng/mL for AQ4N and AQ4M and 2 to 400 ng/mL for AQ4. The assay precision ranged from 6.0% to 8.2% for AQ4N, 3.7% to 4.4% for AQ4M, and 3.6% to 5.3% for AQ4, and was determined to have >92% accuracy. The lower limit of quantification was 2 ng/mL for AQ4 and 10 ng/mL for AQ4N.

Analysis of AQ4 and AQ4N in tissue samples. AQ4N and AQ4 were extracted from tissue samples by homogenizing samples in ice-cold methanol containing 0.2% hydrogen peroxide and centrifuged to precipitate proteins. Supernatants were subjected to high-performance liquid chromatography analysis with detection by diode array and triple quadrupole mass spectrometry (36).

The linear range for the assay based on drug-free H460 xenograft homogenates supplemented with AQ4N or AQ4 was 1 to 1,000 ng/mL for AQ4N and AQ4M and 2 to 400 ng/mL for AQ4. All standards and samples were kept on ice in the dark as a precautionary measure. Stock standards of AQ4N and AQ4 were prepared in 10 mg/mL DMSO and diluted in water. QC samples of AQ4 and AQ4N were prepared from human H460 tumor homogenates at a concentration of 0.5 µg/mL. Accuracy and precision values of <30% were considered acceptable.

Immunohistochemistry. Formalin-fixed, paraffin-embedded tumor sections were dewaxed in xylene and rehydrated using a series of ethanol solutions of increasing dilution. One tissue section was stained with hematoxylin to confirm the presence and quality of tumor. Before staining tissues for Glut-1, 4-µm-thick sections were dewaxed in xylene, passed through graded alcohols to water, exposed to 1% hydrogen peroxide for 30 min at room temperature, and then heated in citrate buffer for 24 min. Sections were incubated for 30 min with 15:1,000 diluted normal goat blocking serum (Vector Laboratories) to minimize nonspecific binding and then incubated with rabbit anti-human Glut-1 antibody (DakoCytomation) at a 1:25 dilution for 90 min at room temperature. Biotinylated anti-rabbit immunoglobulin (Vector Laboratories) as a secondary antibody was applied at 1:200 dilution for 30 min at room temperature followed by incubation with an avidin biotinylated enzyme complex solution (Vectastain, Vector Laboratories) for an additional 30 min at room temperature. Glut-1 antibody on the tissue sections was visualized using 3',3'-diaminobenzidine, and sections were counterstained with hematoxylin solution, dehydrated, and coverslipped. As a negative control, tissues were also stained with a nonimmunized rabbit serum at the same concentrations as the primary antibody.

Sections were viewed at a magnification of ×100 and scored in a blinded fashion by two independent observers according to the proportion of Glut-1 staining (plasma membrane only) in the entire section [0, no staining; 1, light staining (0-5%); 2, medium staining (5-15%); 3, heavy staining (15-30%); and 4, intense staining (>30%)], according to previously published criteria (16). Edge effects, and necrotic and stromal areas were ignored.

Confocal microscopy. Cryosections of 10 to 20 µm thickness were prepared under minimal light exposure and stored at -80°C. Incubations and washes were restricted to minimize potential washout of drug from sections. Sections were fixed in 4% paraformaldehyde for 5 min and washed with PBS. The sections were incubated for 5 min

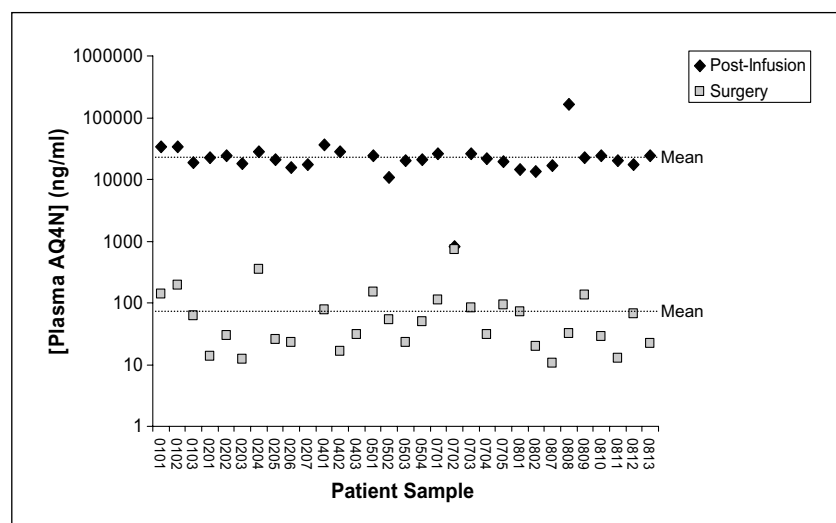


Fig. 1. Plasma levels of AQ4N immediately following infusion and at time of surgery. Plasma concentrations of AQ4N (ng/mL) from individual patients immediately after dosing (*solid diamonds*) and immediately before surgical resection (*shaded squares*).

with anti-Glut-1 antibody (GT12-A, Alpha Diagnostics, Inc.), detected with a Alexa Flour 488-conjugated anti-rabbit secondary or with a mouse monoclonal anti-GFAP-Alexa Fluor 488 conjugate (Invitrogen). Antibodies were diluted in PBS containing 0.25% (v/v) fish skin gelatin (Sigma). Following three brief PBS washes, samples were mounted using an aqueous mountant with 4',6-diamidino-2-phenylindole (DAPI; Vector Laboratories) and imaged on a Zeiss LSM 510 meta-confocal microscope using a 633-nm laser to excite AQ4 fluorescence as described previously (40). $\times 40$ and $\times 63$ objectives were used with up to $5\times$ digital zoom as needed for each section. Differential interference contrast imaging was used to detect cytoplasmic blebbing indicative of apoptosis (41). Projected z-stacks were rendered using Volocity three-dimensional imaging software (Improvision).

Statistical analysis. All statistical analysis was done using a two-tailed Student's *t* test using GraphPad Prism software (GraphPad Software, Inc.). A *P* value of <0.05 was considered to be statistically significant.

Results

Thirty-three patients from six centers in United Kingdom and Latvia were enrolled between November 2004 and September 2005, of whom 32 received AQ4N and completed the study. One patient enrolled in the study experienced a myocardial infarction before surgery and was withdrawn from the study. All subjects had solid tumors that required surgical resections of the following indications: GBM ($n = 8$), head and neck carcinoma ($n = 8$), bladder carcinoma ($n = 9$), breast carcinoma ($n = 6$), and cervical carcinoma ($n = 1$). Most patients on the study were treatment naive with the exception of two bladder carcinoma patients who received either prior Bacillus Calmette-Guerin or radiation treatment and one head and neck carcinoma patient who received prior radiation therapy. Other patient characteristics are shown in Supplementary Table S1.

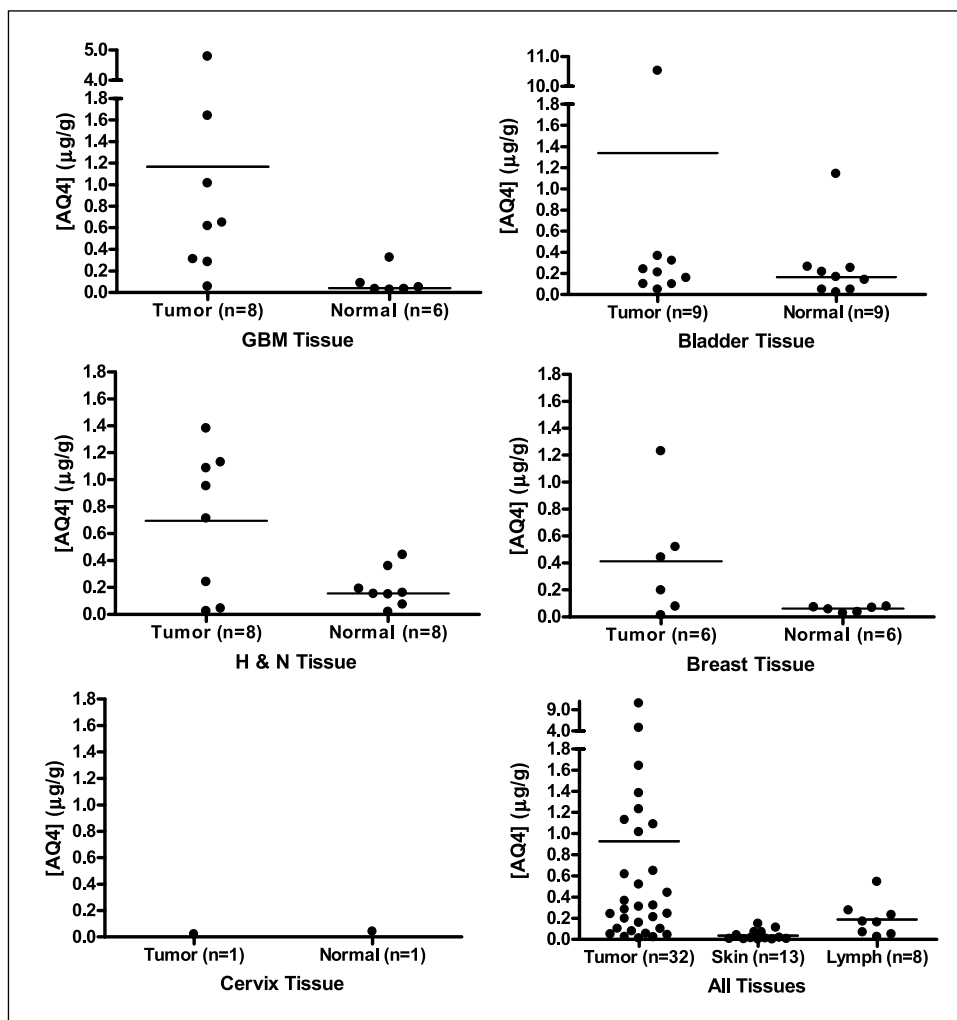
Plasma and tissue levels of drug. Immediately before the end of drug infusion, the mean (\pm SE) levels of AQ4N in the plasma were 26.2 ± 4.8 μ g/mL (Fig. 1). Plasma levels of the activated metabolite, AQ4, following drug infusion represented $<0.04\%$ of AQ4N levels measured (Supplementary Table S2). At the time of surgery, AQ4N plasma levels were very low (89.8 ± 25.0 ng/mL) and represented $<0.4\%$ of AQ4N levels measured following infusion (Fig. 1) and there was no significant correlation between the time interval between infusion and

surgery, and AQ4N levels before surgery (data not shown). This confirms previous observations from clinical studies indicating the rapid clearance of AQ4N from the systemic circulation (36, 37). Importantly, the fully bioreduced AQ4 metabolite could not be detected from the plasma at the time of surgery in 29 of 32 samples (Supplementary Table S2). Thus, little if any AQ4N or AQ4 was present systemically when tumor and normal tissue samples were taken, minimizing the possibility of contamination from blood.

Ninety-five biopsy samples from 32 patients were analyzed for AQ4N and AQ4 concentrations. Normal tissue samples adjacent to the tumor were harvested in 30 of 32 patients as well as distal skin (13 patients) and lymph nodes (8 patients). The bioreduced AQ4 metabolite was detected in all tumor samples, in most cases at higher concentrations than in the corresponding normal tissues, demonstrating tumor activation of the prodrug in man (Fig. 2; Supplementary Table S3). The mean (\pm SE) tumor concentration of AQ4 from all patients was 0.93 ± 0.37 μ g/g, compared with mean (\pm SE) normal tissue concentrations of 0.15 ± 0.05 μ g/g, demonstrating clear tumor selectivity ($P = 0.04$). In contrast, AQ4N was only detected in 11 of 32 tumor samples and predominantly in bladder tissues. The mean tissue concentrations of AQ4 and AQ4N for each tumor type and the mean concentration ratios of tumor to normal are shown in Table 1. The mean AQ4 tumor to normal ratio for the majority of tumor types ranged from 3.1 to 19.2, clearly demonstrating targeting of the cytotoxic metabolite to tumor tissue (Table 1). The only exception was the single patient with cervical cancer who had an AQ4 tumor to normal ratio of 0.5.

Variability of AQ4 levels within tumors was noted in this study. For example, in one GBM patient, nine samples from multiple sites within the tumor had AQ4 levels that ranged from 0.034 to 0.65 μ g/g, with six of the nine samples having concentrations that exceeded 0.2 μ g/g. Similarly, a bladder tumor specimen from one patient contained AQ4 at a concentration of 10.5 μ g/g, which was ~ 30 -fold higher than the highest value of the other nine patients (Fig. 2). In three bladder cancer patients, AQ4 levels in normal tissue exceeded those in the corresponding tumor tissue. AQ4N was detected in the majority of bladder tumor samples, in contrast with other tissues studied. In two of six breast tumor patients, it was

Fig. 2. Levels of bio-reduced AQ4 metabolite in tumor and normal tissues. AQ4 concentrations ($\mu\text{g/g}$) from resected tumors and corresponding adjacent normal tissues from patients with GBM ($n = 8$), bladder ($n = 9$), head and neck ($n = 8$), breast ($n = 6$), and cervix ($n = 1$) cancers. AQ4 was also measured in distal normal skin samples ($n = 13$) and lymph nodes ($n = 8$), when available.



observed that lymph node specimens had relatively high levels of AQ4 (Supplementary Table S3). For one GBM and two head and neck patients, tumor samples from both peripheral and internal regions of the tumor had higher AQ4 concentrations in the central regions of the tumors.

Hypoxia detection by immunohistochemistry. To assess the level of hypoxia in the biopsy samples, we elected to measure the expression of Glut-1, an endogenous marker of tumor

hypoxia (15–19). A total of 70 biopsy samples from 30 patients were assessed by immunohistochemistry for Glut-1, to assess the level of hypoxia within a section. Many tumor sections displayed clear and extensive regions of Glut-1+ hypoxic cells in contrast to the majority of normal tissue demonstrating little or no staining (Fig. 3; Supplementary Table S4). The mean percentage of Glut-1+ cells for each tumor type, except cervix, ranged from 11% to 46% ($n = 28$) in tumor

Table 1. Mean (\pm SE) levels of AQ4 and AQ4N ($\mu\text{g/g}$) in tumor and normal samples

Tissue (n)	AQ4 ($\mu\text{g/g}$)*			AQ4N ($\mu\text{g/g}$)		
	Tumor	Adjacent normal	T:N ratio [†]	Tumor	Adjacent normal	T:N ratio [†]
GBM (8)	1.17 \pm 0.54	0.09 \pm 0.05	19.2	0.10 \pm 0.09	0.04 \pm 0.01	2.46
Bladder (9)	1.34 \pm 1.15	0.25 \pm 0.11	8.5	8.41 \pm 8.05	0.14 \pm 0.07	61.2
Head and neck (8)	0.69 \pm 0.19	0.19 \pm 0.05	3.1	BLQ	BLQ	NA
Breast (6)	0.41 \pm 0.18	0.05 \pm 0.01	6.9	BLQ	BLQ	NA
Cervix (1)	0.02	0.04	0.5	BLQ	BLQ	NA
Skin (13)	—	0.04 \pm 0.01	—	—	0.02 \pm 0.01	—
Lymph (8)	—	0.19 \pm 0.06	—	—	0.01 \pm 0.01	—

Abbreviations: BLQ, below limit of quantification; T:N, tumor to normal ratio; NA, not applicable.

*Where more than one tumor sample was assayed for a patient, mean interpatient tumor values for those patients were used.

[†] Mean of tumor to normal ratios for individual patients.

tissues in contrast to only 0% to 0.5% being observed in normal tissues ($n = 21$; $P < 0.05$; Supplementary Table S4). In general, tumor sections with considerable Glut-1 staining had higher levels of AQ4, whereas sections with little or no staining contained little AQ4 (Figs. 3 and 4). When samples were classified into three levels of AQ4 concentration, low ($<0.2 \mu\text{g/g}$), medium ($0.2\text{--}1 \mu\text{g/g}$), and high ($>1 \mu\text{g/g}$), AQ4 tumor concentrations correlated with increased tumor hypoxia as assessed by Glut-1+ staining (Fig. 4A). The mean ($\pm\text{SE}$) Glut-1 percentages for tissues classified as possessing high ($>1 \mu\text{g/g}$) AQ4 levels were significantly higher than those expressing low ($<0.2 \mu\text{g/g}$) AQ4 (46.4 ± 10.3 versus 3.2 ± 1.6 , $P < 0.001$; Fig. 4A), consistent with preferential activation of AQ4N within the more hypoxic regions. Similarly, sections possessing $>15\%$ Glut-1+ regions (scored 3 and 4) were observed to contain significantly higher mean AQ4 levels than nonhypoxic tissues with no Glut-1 expression (1.64 ± 0.76 versus $0.13 \pm 0.04 \mu\text{g/g}$, $P < 0.005$; Fig. 4B).

Correlation of Glut-1 and AQ4 by confocal microscopy. The Glut-1 immunohistochemistry provided evidence for an association between levels of AQ4 in tumors and the degree of hypoxia. We investigated this further by exploiting the intrinsic fluorescence of AQ4 (40), which allows the drug to be visualized in tumor sections using confocal microscopy. A total of seven tumor samples from five patients with GBM ($n = 2$), bladder ($n = 1$), head and neck ($n = 1$), and breast ($n = 1$) cancers were analyzed by confocal microscopy and immunofluorescence.

AQ4-associated fluorescence was detected in two of four GBM samples from two patients, and in each of the bladder and head and neck tumor samples. In all samples examined, AQ4 fluorescence was restricted within regions expressing the highest levels of Glut-1+ (Fig. 5A-C). In one patient with bladder cancer who had a high intratumoral concentration of AQ4 ($10.5 \mu\text{g/g}$), there was clear nuclear localization of AQ4, which related closely to microregions of Glut-1+ cells (Fig. 5A). In most other samples, AQ4-associated fluorescence accumulated in heterogeneous speckles (Fig. 5B and C). AQ4 was also

detected in areas that lacked cellular architecture on differential interference contrast imaging and nuclear DAPI staining, features consistent with necrosis (Fig. 5 and data not shown). In some cells peripheral to these necrotic regions, AQ4 was found at high levels in cells exhibiting morphologic features of apoptosis, including nuclear fragmentation and cytoplasmic blebbing (Fig. 5D and data not shown).

Toxicity. In general, AQ4N was well tolerated. No deaths occurred during the 30-day study period. Twenty-five patients experienced a total of 99 adverse events, the majority of which were mild to moderate in intensity. The most common adverse events that occurred following treatment ($\geq 10\%$) included nausea, postprocedural pain, headache, skin discoloration, hypertension, hypotension, and pyrexia. The adverse events that were considered likely to be drug related were generalized gray/blue skin discoloration (seven adverse events) and fatigue (two adverse events). No hematologic toxicities were noted. Three patients experienced four serious adverse events. One patient with a history of ischemic heart disease experienced a myocardial infarction and left ventricular failure, which were both considered to be possibly drug related by the treating physician. The other two serious adverse events in two other patients, worsening obstructive airways disorder and severe postoperative infection, were not considered to be drug related. All of these serious adverse events resolved.

Discussion

The key finding of this study has been to confirm the tumor selectivity and hypoxia targeting of AQ4N in man. Our data clearly show that the activated form of the prodrug, AQ4, preferentially accumulates in tumor rather than in normal tissues, is present at higher levels in tumors with greater degrees of hypoxia, and seems to be localized within regions comprising hypoxic tumor cells. This is the first time, to our knowledge, that the activation of a bio-reductive agent in clinical tumor samples has been shown.

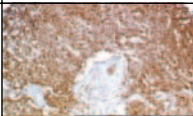
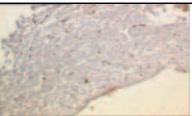
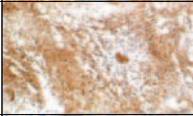
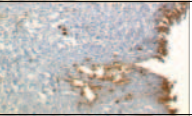

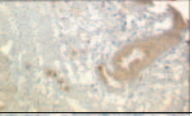

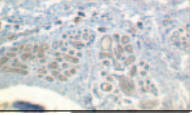
ID #	Disease	Tumor Tissue	Glut1 %	[AQ4] ($\mu\text{g/g}$)	Normal Tissue	Glut1 %	[AQ4] ($\mu\text{g/g}$)
0204	GBM		90	1.01		0	0.09
0707	Bladder		80	10.52		0	0.16
0801	H & N		40	1.09		0	0.15
0807	Breast		6.2	0.52		2.5	0.08

Fig. 3. Representative biopsy samples for Glut-1 hypoxia marker and AQ4 levels. Representative sections from GBM, bladder, head and neck, and breast tumor samples and corresponding normal tissue sections analyzed for Glut-1 expression (brown staining) following immunohistochemical staining; approximate percentage of Glut-1+ regions for each section is shown beside each image. Concentrations of AQ4 ($\mu\text{g/g}$) for each tumor sample are shown beside the % Glut-1 scores.

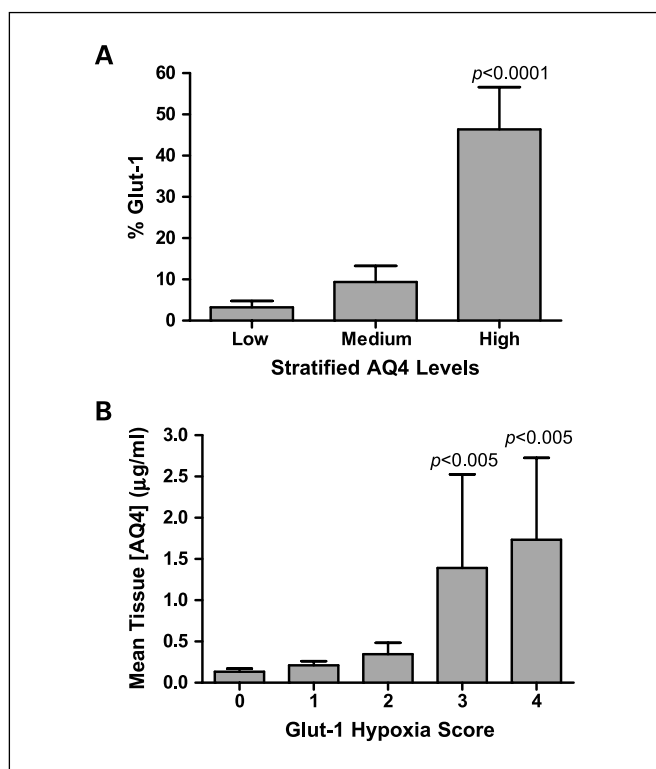


Fig. 4. Correlation of tumor hypoxia (Glut-1 staining) and AQ4. *A*, percentage of Glut-1+ regions for each section plotted against tissue samples that contained low (0-0.2 µg/g), medium (0.2-1 µg/g), or high (>1 µg/g) AQ4 concentrations. Columns, mean; bars, SE. *B*, AQ4 tissue levels plotted against Glut-1 score. Columns, mean; bars, SE. Glut-1 score: 0, no staining; 1, 0% to 5% Glut-1+; 2, 5% to 15% Glut-1+; 3, 15% to 30% Glut-1+; 4, >30% Glut-1+.

AQ4N was designed to be an inactive prodrug in most healthy tissues but would be selectively activated to a potent cytotoxin in hypoxic regions that are characteristic of many solid tumors. Previous clinical trials have indeed shown that AQ4N is well tolerated in patients without evidence of any major systemic toxicities at doses up to 768 mg/m² given weekly as a single agent (37) or 447 mg/m² when given in combination with radiotherapy (36). The traditional paradigm for anticancer drug development would then be to undertake a broad program of empirical phase II trials with tumor shrinkage as the primary end point. This is, however, not optimal for rationally designed agents. Moreover, the targeting of hypoxic areas of tumors by AQ4N may not achieve sufficient tumor debulking to satisfy conventional Response Evaluation Criteria in Solid Tumors (43). Therefore, proof-of-principle studies are vital if novel agents are to be developed rationally. A previous phase I study of AQ4N and radiotherapy provided preliminary data suggesting that AQ4 was generated preferentially in esophageal cancers (36). There remained, however, a need to show this effect definitively in patients with a spectrum of tumors receiving AQ4N as a single agent, and to define the relationship between tumor hypoxia and the accumulation of the activated form of this prodrug.

The bioreduced, cytotoxic metabolite AQ4 was detected in all tumor samples; the mean tumor to normal ratio for AQ4 in the majority of tumor types ranged from 3.1 to 19.2, demonstrating clear tumor selective activation. The only exception was a single patient with cervical cancer who had a ratio of 0.5. By contrast,

tumor to normal ratios of AQ4 were particularly high in GBM (mean 19.2). These data show that AQ4N effectively traverses the blood-brain barrier and is selectively activated in GBM. The absence of AQ4N bioactivation in normal tissues or in the circulation is ideal for an anticancer prodrug and is consistent with earlier reports demonstrating that AQ4N is well tolerated in patients with solid tumor malignancies (36, 37).

Based on our immunohistochemical data, tumor biopsies almost certainly included normoxic cells, suggesting that these mean tumor concentrations of AQ4 most likely underestimate the concentrations present in hypoxic areas of the tumors. In addition, hypoxia is a dynamic process and is dependent on both tumor vascularization and growth. The heterogeneity of hypoxia would be expected to result in considerable variation in the amounts of AQ4 generated in different regions of a tumor. Interestingly, one patient had a 20-fold variance in AQ4 concentration in nine samples from the same tumor; in three other cases where multiple samples of the same tumor were analyzed, the central portion of the tumor had higher concentrations of AQ4 than the peripheral area. This is consistent with the expected regional differences in hypoxia, although this hypothesis was not directly tested.

Whereas AQ4 was prevalent in tumor tissues, AQ4N was only detected in 11 of 32 tumor samples and predominantly in bladder tissues. At the time of surgery, AQ4N plasma levels were very low, confirming previous observations of rapid AQ4N clearance from the systemic circulation (36, 37); the fully bioreduced AQ4 metabolite could be detected in plasma at the time of surgery in only 3 of 32 samples. With little, if any, AQ4N or AQ4 present in the plasma at surgery, the possibility of contamination of tumor and normal tissue samples by blood is minimized. Because AQ4N is eliminated through the kidneys, AQ4N-rich urine bathes the bladder walls for some hours following administration and may contribute to the "atypical" AQ4N accumulation in bladder cancer patients observed in this study.

Having shown tumor selective activation of AQ4, we wanted to establish that this was mediated by tumor hypoxia. Although the clinical importance of hypoxia is widely recognized, there remains controversy regarding how hypoxia is best quantified (42). We elected to use an endogenous marker of hypoxia rather than an exogenous bioreductive marker such as pimonidazole to minimize the risk of any interaction between test agents. Glut-1 is well recognized to be regulated by hypoxia and there are numerous studies demonstrating its utility as a marker of endogenous hypoxia as well as its association with tumor aggressiveness and poor prognosis in a variety of neoplasms (15-19, 44). The presence of Glut-1 is likely to represent chronic hypoxia and may underrepresent transient hypoxic episodes that frequently occur in tumors due to high interstitial pressures and temporary vascular occlusion. We would, however, expect AQ4N to be equally activated under transient or chronic hypoxia, which may reduce the correlation with Glut-1 staining. Therefore, the significant increase ($P < 0.001$) in Glut-1 staining in tumor samples compared with normal tissue, and the clear association between increased tissue AQ4 levels and high Glut-1 staining both support the assertion that AQ4 is selectively activated in hypoxic tumors. This conclusion was further supported by confocal microscopy, where direct colocalization of AQ4 in hypoxic regions was observed. These results are consistent with preclinical evidence

demonstrating tumor-hypoxia targeting of AQ4N in xenograft models (28, 45–47).

The hypoxia-dependent activation of AQ4N also requires the bioreductive activity of certain CYP enzymes (30, 31, 35). Although some CYP isoforms, such as CYP 3A4, have been shown to activate AQ4N more efficiently than others, multiple CYP enzymes are capable of contributing to prodrug activation (30, 31, 35, 48–50). Hence, we did not choose to assay the biopsy samples for the expression of individual CYP enzymes. A separate study has shown that microsome extracts from 20

clinical brain tumor specimens expressed different complements of CYP enzymes and could all activate AQ4N *ex vivo* under anoxia, albeit with different efficiency (35). The observation of high levels of AQ4 in multiple tumor samples after a single administration of AQ4N does not suggest that CYP expression is likely to be a limiting factor in the effectiveness of AQ4N therapy.

In this study, single 200 mg/m² doses of AQ4N were well tolerated. This dose was selected based on a number of criteria. Previous clinical studies have confirmed that doses of up to 447

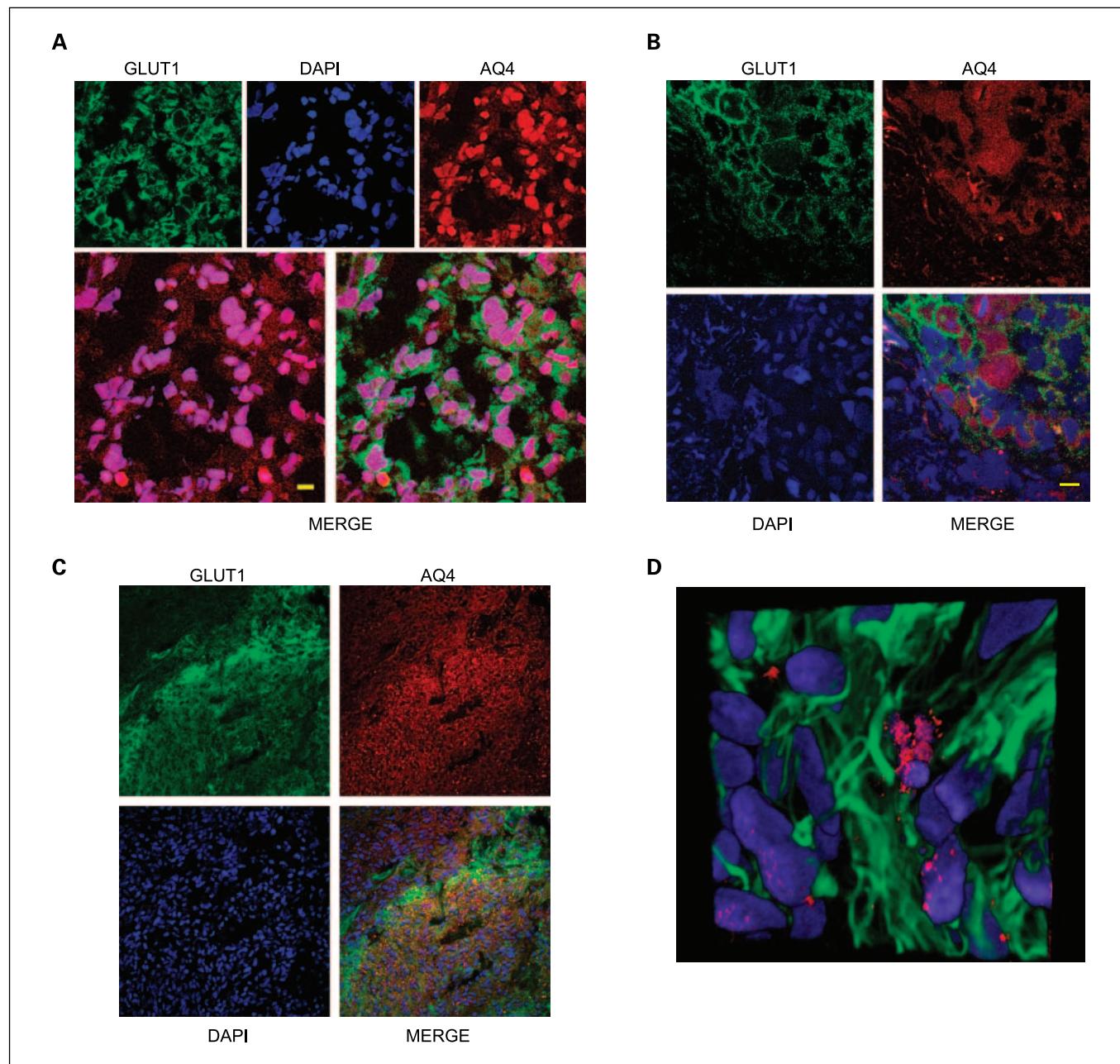


Fig. 5. AQ4 colocalizes with Glut-1+ hypoxic tumor regions. Representative tumor sections analyzed by confocal microscopy. *A* to *C*, Glut-1+ staining (green), DAPI tumor nuclei (blue), and AQ4-dependent fluorescence (red). *D*, glial fibrillary acidic protein tumor marker (green), AQ4 (red), and DAPI (blue). Scale bars (yellow), 10 μ m. *A*, bladder tumor (sample 0707). Bottom left, an overlay of AQ4 and DAPI nuclear stain; bottom right, a merged image of Glut-1+, DAPI+, and AQ4+ sections. *B*, head and neck tumor (sample 801). Bottom right, merged image of all three sections demonstrating colocalization of AQ4 drug within hypoxic Glut-1+ tumor regions. *C*, GBM tumor (sample 0503). Bottom right, merged image of all three sections demonstrating colocalization of AQ4 drug within hypoxic Glut-1+ tumor regions. *D*, GBM tumor (sample 0503). Reconstructed three-dimensional z-stack image demonstrating AQ4 abundance in cells undergoing nuclear fragmentation, overlaying AQ4, DAPI, and GFAP.

and 768 mg/m² are safe and well tolerated (36, 37), so the 200 mg/m² dose gave a considerable safety margin in the presurgical setting, where AQ4N had not previously been evaluated. Full pharmacokinetic profiles were not obtained in the current study, but in an earlier study a single AQ4N dose of 176 mg/m² had area-under-the-curve values of 46 to 86 µg·h/mL (36). This compares with plasma area under the curve of 50 µg·h/mL in mice receiving 60 mg/kg of AQ4N, a dose that has been shown to be efficacious in xenograft models and that resulted in intratumoral AQ4 levels of 0.2 to 1.0 µg/g (47). In this present clinical study, intratumoral AQ4 levels were observed to be >0.2 µg/g in 30 of 32 patients (>90%), further supporting the view that this dose may be potentially therapeutic. Because we could not obtain serial tumor samples, it was not possible to assess the kinetics of intratumoral AQ4 formation.

Taken together, these observations show that the low toxicity prodrug AQ4N is converted to the active metabolite AQ4 in hypoxic regions of tumors in man. Nevertheless, a number of questions cannot be answered by the current study. First, we do not know whether this will translate into enhanced therapeutic benefit in patients with cancer. Second, it is unclear whether the 200 mg/m² dose explored in this study is optimal. Third, it is unknown whether patients with more hypoxic tumors will

achieve a better therapeutic outcome following AQ4N treatment. This final question may be important in selecting patients for future trials, but it is encouraging that selective activation of AQ4N in significant areas of hypoxia were seen in most tumors types studied. The current study provides a strong rationale for trials addressing these and other questions.

In summary, we have shown proof-of-concept for the preferential activation of AQ4N in hypoxic compartments of several important solid tumors, leading to potentially therapeutic levels of a potent topoisomerase II poison in regions of the tumor microenvironment that are typically refractory to conventional chemotherapy and radiotherapy. In addition, this study also confirmed that AQ4N effectively crosses the blood-brain barrier, resulting in high levels of the activated AQ4 metabolite within primary brain tumors. These data encourage the further clinical development of AQ4N for the treatment of solid tumors including GBM.

Acknowledgments

We thank all the clinical centers, investigators, and patients that participated in this study; James Taylor and Beryl Cronin (Institute of Cancer Therapeutics, Bradford, United Kingdom) for their technical expertise; and the National Translational Cancer Research Network for their support in this study.

References

- Harris AL. Hypoxia—a key regulatory factor in tumour growth. *Nat Rev Cancer* 2002;2:38–47.
- Brown JM, Giaccia AJ. The unique physiology of solid tumors: opportunities (and problems) for cancer therapy. *Cancer Res* 1998;58:1408–16.
- Hockel M, Vaupel P. Tumor hypoxia: definitions and current clinical, biologic, and molecular aspects. *J Natl Cancer Inst* 2001;93:266–76.
- Brown JM, Wilson WR. Exploiting tumour hypoxia in cancer treatment. *Nat Rev Cancer* 2004;4:437–47.
- Le QT, Denko NC, Giaccia AJ. Hypoxic gene expression and metastasis. *Cancer Metastasis Rev* 2004;23:293–310.
- Erler JT, Bennewith KL, Nicolau M, et al. Lysyl oxidase is essential for hypoxia-induced metastasis. *Nature* 2006;440:1222–6.
- Chi JT, Wang Z, Nuyten DS, et al. Gene expression programs in response to hypoxia: cell type specificity and prognostic significance in human cancers. *PLoS Med* 2006;3:e47.
- Hockel M, Schlenger K, Mitze M, Schaffer U, Vaupel P. Hypoxia and radiation response in human tumors. *Semin Radiat Oncol* 1996;6:3–9.
- Minchinton AI, Tannock IF. Drug penetration in solid tumours. *Nat Rev Cancer* 2006;6:583–92.
- Shannon AM, Bouchier-Hayes DJ, Condron CM, Toomey D. Tumour hypoxia, chemotherapeutic resistance and hypoxia-related therapies. *Cancer Treat Rev* 2003;29:297–307.
- Vaupel P, Mayer A. Hypoxia in cancer: significance and impact on clinical outcome. *Cancer Metastasis Rev* 2007;26:225–39.
- Young SD, Marshall RS, Hill RP. Hypoxia induces DNA overreplication and enhances metastatic potential of murine tumor cells. *Proc Natl Acad Sci U S A* 1988;85:9533–7.
- Graeber TG, Osmanian C, Jacks T, et al. Hypoxia-mediated selection of cells with diminished apoptotic potential in solid tumours. *Nature* 1996;379:88–91.
- Comerford KM, Wallace TJ, Karhausen J, Louis NA, Montalto MC, Colgan SP. Hypoxia-inducible factor-1-dependent regulation of the multidrug resistance (MDR1) gene. *Cancer Res* 2002;62:3387–94.
- Airley R, Loncaster J, Davidson S, et al. Glucose transporter glut-1 expression correlates with tumor hypoxia and predicts metastasis-free survival in advanced carcinoma of the cervix. *Clin Cancer Res* 2001;7:928–34.
- Hoskin PJ, Sibtain A, Daley FM, Wilson GD. GLUT1 and CAIX as intrinsic markers of hypoxia in bladder cancer: relationship with vascularity and proliferation as predictors of outcome of ARCON. *Br J Cancer* 2003;89:1290–7.
- Jonathan RA, Wijffels KI, Peeters W, et al. The prognostic value of endogenous hypoxia-related markers for head and neck squamous cell carcinomas treated with ARCON. *Radiother Oncol* 2006;79:288–97.
- Mellanen P, Minn H, Grenman R, Harkonen P. Expression of glucose transporters in head-and-neck tumors. *Int J Cancer* 1994;56:622–9.
- Kato H, Takita J, Miyazaki T, et al. Glut-1 glucose transporter expression in esophageal squamous cell carcinoma is associated with tumor aggressiveness. *Anticancer Res* 2002;22:2635–9.
- Patterson LH, McKeown SR. AQ4N: a new approach to hypoxia-activated cancer chemotherapy. *Br J Cancer* 2000;83:1589–93.
- Patterson LH. Bioreductively activated antitumor N-oxides: the case of AQ4N, a unique approach to hypoxia-activated cancer chemotherapy. *Drug Metab Rev* 2002;34:581–92.
- McKeown SR, Hejmadi MV, McIntyre IA, McAleer JJ, Patterson LH. AQ4N: an alkylaminoanthraquinone N-oxide showing bioreductive potential and positive interaction with radiation *in vivo*. *Br J Cancer* 1995;72:76–81.
- McKeown SR, Cowen RL, Williams KJ. Bioreductive drugs: from concept to clinic. *Clin Oncol (R Coll Radiol)* 2007;19:427–42.
- McKeown SR, Friery OP, McIntyre IA, Hejmadi MV, Patterson LH, Hirst DG. Evidence for a therapeutic gain when AQ4N or tirapazamine is combined with radiation. *Br J Cancer Suppl* 1996;27:S39–42.
- Patterson LH, McKeown SR, Ruparella K, et al. Enhancement of chemotherapy and radiotherapy of murine tumours by AQ4N, a bioreductively activated anti-tumour agent. *Br J Cancer* 2000;82:1984–90.
- Gallagher R, Hughes CM, Murray MM, et al. The chemopotential of cisplatin by the novel bioreductive drug AQ4N. *Br J Cancer* 2001;85:625–9.
- Friery OP, Gallagher R, Murray MM, et al. Enhancement of the anti-tumour effect of cyclophosphamide by the bioreductive drugs AQ4N and tirapazamine. *Br J Cancer* 2000;82:1469–73.
- Tredan O, Lalani AS, Garber AS, Tannock IF. The hypoxia-activated prodrug, AQ4N, penetrates deeply in tumor tissues and complements the limited distribution of mitoxantrone. *Proc Am Assoc Cancer Res* 2007;48:1356.
- Smith PJ, Blunt NJ, Desnoyers R, Giles Y, Patterson LH. DNA topoisomerase II-dependent cytotoxicity of alkylaminoanthraquinones and their N-oxides. *Cancer Chemother Pharmacol* 1997;39:455–61.
- Raleigh SM, Wanogho E, Burke MD, Patterson LH. Rat cytochromes P450 (CYP) specifically contribute to the reductive bioactivation of AQ4N, an alkylaminoanthraquinone-di-N-oxide anticancer prodrug. *Xenobiotica* 1999;29:1115–22.
- Raleigh SM, Wanogho E, Burke MD, McKeown SR, Patterson LH. Involvement of human cytochromes P450 (CYP) in the reductive metabolism of AQ4N, a hypoxia activated anthraquinone di-N-oxide prodrug. *Int J Radiat Oncol Biol Phys* 1998;42:763–7.
- Patterson LH, McKeown SR, Robson T, Gallagher R, Raleigh SM, Orr S. Antitumour prodrug development using cytochrome P450 (CYP) mediated activation. *Anticancer Drug Des* 1999;14:473–86.
- Patterson LH, Murray GI. Tumour cytochrome P450 and drug activation. *Curr Pharm Des* 2002;8:1335–47.
- Rooney PH, Telfer C, McFadyen MC, Melvin WT, Murray GI. The role of cytochrome P450 in cytotoxic bioactivation: future therapeutic directions. *Curr Cancer Drug Targets* 2004;4:257–65.
- Wu HJ, Zhao J, Liu SS, Ding L, Yang DL. Metabolism of AQ4N in primary and metastatic brain tumor microsomes. *China Med Eng* 2006;14:590–4.
- Steward WP, Middleton M, Benghiat A, et al. The use of pharmacokinetic and pharmacodynamic endpoints to determine the dose of AQ4N, a novel hypoxic cell cytotoxin, given with fractionated radiotherapy in a phase I study. *Ann Oncol* 2007;18:1098–103.

37. Sarantopoulos J, Tolcher AW, Wong A, et al. Banoxantrone (AQ4N), tissue CYP 450 targeted prodrug: The results of a phase I study using an accelerated dose escalation. *JCO Suppl* 2006;24:81s.
38. Loadman PM, Swaine DJ, Bibby MC, Welham KJ, Patterson LH. A preclinical pharmacokinetic study of the bioreductive drug AQ4N. *Drug Metab Dispos* 2001;29:422–6.
39. Swaine DJ, Loadman PM, Bibby MC, Graham MA, Patterson LH. High-performance liquid chromatographic analysis of AQ4N, an alkylaminoanthraquinone N-oxide. *J Chromatogr B Biomed Sci Appl* 2000;742:239–45.
40. Smith PJ, Desnoyers R, Blunt N, Giles Y, Patterson LH, Watson JV. Flow cytometric analysis and confocal imaging of anticancer alkylaminoanthraquinones and their N-oxides in intact human cells using 647-nm krypton laser excitation. *Cytometry* 1997;27:43–53.
41. Coleman ML, Sahai EA, Yeo M, Bosch M, Dewar A, Olson MF. Membrane blebbing during apoptosis results from caspase-mediated activation of ROCK I. *Nat Cell Biol* 2001;3:339–45.
42. Vordermark D, Brown JM. Endogenous markers of tumor hypoxia predictors of clinical radiation resistance? *Strahlenther Onkol* 2003;179:801–11.
43. Michaelis LC, Ratain MJ. Measuring response in a post-RECIST world: from black and white to shades of grey. *Nat Rev Cancer* 2006;6:409–14.
44. Palit V, Phillips RM, Puri R, Shah T, Bibby MC. Expression of HIF-1 α and Glut-1 in human bladder cancer. *Oncol Rep* 2005;14:909–13.
45. Lalani AS, Alters SE, Wong A, Albertella MR, Cleland JL, Henner WD. Selective tumor targeting by the hypoxia-activated prodrug AQ4N blocks tumor growth and metastasis in preclinical models of pancreatic cancer. *Clin Cancer Res* 2007;13:2216–25.
46. Atkinson SJ, Loadman PM, Sutton C, Patterson LH, Clench MR. Examination of the distribution of the bioreductive drug AQ4N and its active metabolite AQ4 in solid tumours by imaging matrix-assisted laser desorption/ionisation mass spectrometry. *Rapid Commun Mass Spectrom* 2007;21:1271–6.
47. Albertella MR, Loadman PM, Williams KJ, et al. *In vivo* activation of the hypoxia-targeted cytotoxin AQ4N in human tumour xenografts. *Proc Am Assoc Cancer Res* 2006;47:314.
48. McCarthy HO, Yakkundi A, McErlane V, et al. Bioreductive GDEPT using cytochrome P450 3A4 in combination with AQ4N. *Cancer Gene Ther* 2003;10:40–8.
49. McErlane V, Yakkundi A, McCarthy HO, et al. A cytochrome P450 2B6 mediated gene therapy strategy to enhance the effects of radiation or cyclophosphamide when combined with the bioreductive drug AQ4N. *J Gene Med* 2005;7:851–9.
50. Yakkundi A, McErlane V, Murray M, et al. Tumor-selective drug activation: a GDEPT approach utilizing cytochrome P450 1A1 and AQ4N. *Cancer Gene Ther* 2006;13:598–605.

Clinical Cancer Research

Hypoxia-Selective Targeting by the Bioreductive Prodrug AQ4N in Patients with Solid Tumors: Results of a Phase I Study

Mark R. Albertella, Paul M. Loadman, Philip H. Jones, et al.

Clin Cancer Res 2008;14:1096-1104.

Updated version	Access the most recent version of this article at: http://clincancerres.aacrjournals.org/content/14/4/1096
Supplementary Material	Access the most recent supplemental material at: http://clincancerres.aacrjournals.org/content/suppl/2008/02/18/14.4.1096.DC1

Cited articles	This article cites 50 articles, 6 of which you can access for free at: http://clincancerres.aacrjournals.org/content/14/4/1096.full#ref-list-1
Citing articles	This article has been cited by 13 HighWire-hosted articles. Access the articles at: http://clincancerres.aacrjournals.org/content/14/4/1096.full#related-urls

E-mail alerts	Sign up to receive free email-alerts related to this article or journal.
Reprints and Subscriptions	To order reprints of this article or to subscribe to the journal, contact the AACR Publications Department at pubs@aacr.org .
Permissions	To request permission to re-use all or part of this article, use this link http://clincancerres.aacrjournals.org/content/14/4/1096 . Click on "Request Permissions" which will take you to the Copyright Clearance Center's (CCC) Rightslink site.